

Research paper

Noninvasive and quantitative measurement of C4d deposition for the diagnosis of antibody-mediated cardiac allograft rejection



Tao Liao ^{a,1}, Xiaonan Liu ^{a,1}, Jie Ren ^{b,1}, Hongjun Zhang ^b, Haofeng Zheng ^a, Xiujie Li ^c, Yannan Zhang ^a, Fei Han ^a, Tinghui Yin ^b, QiQuan Sun ^{a,*}

^a Organ Transplantation Research Institute of Sun Yat-sen University, the Third Affiliated Hospital of Sun Yat-sen University, Guangzhou, Guangdong, China

^b Department of Medical Ultrasound, the Third Affiliated Hospital of Sun Yat-sen University, Guangzhou, Guangdong, China

^c Department of Obstetrics and Gynecology, the Third Affiliated Hospital of Sun Yat-sen University, Guangzhou, Guangdong, China

ARTICLE INFO

Article history:

Received 15 August 2018

Received in revised form 15 October 2018

Accepted 24 October 2018

Available online 29 October 2018

Keywords:

Noninvasive

Antibody-mediated rejection

C4d

Cardiac transplantation

Targeted microbubbles

ABSTRACT

Background: C4d is a specific biomarker for the diagnosis of antibody-mediated rejection (AMR) after cardiac transplantation. Although strongly recommended, routine C4d surveillance is hindered by the invasive nature of endomyocardial biopsy. Targeted ultrasound (US) has high sensitivity, and C4d is abundantly expressed within the graft of patients experiencing AMR, which makes it possible to visualize C4d deposition in vivo using targeted US.

Methods: We designed a serial dilution of C4d-targeted microbubbles (MB_{C4d}) using a streptavidin-biotin conjugation system. A rat model of AMR with C4d deposition was established by pre-sensitization with skin transplantation before cardiac transplantation. MB_{C4d} were injected into recipients and then qualitatively and quantitatively analyzed using the destruction-replenishment method with a clinical US imaging system and analyzed by software.

Findings: We successfully obtained qualitative images of C4d deposition in a wide cardiac allograft section, which, for the first time, reflected real-time C4d distribution. Moreover, normal intensity difference was used for quantitative analysis and exhibited an almost nearly linear correlation with the grade of C4d deposition according to the pathologic evidence. In addition, MB_{C4d} injection did not affect the survival and aggravate injury, which demonstrates its safety.

Interpretation: This study demonstrates a noninvasive, quantitative and safe evaluation method for C4d. As contrast-enhanced US has been widely used in clinical settings, this technology is expected to be applied quickly to clinical practice.

Fund: National Natural Science Foundation of China and Guangdong Province, Leading Scientific Talents of Guangdong special support program, the Science and Technology Project of Guangdong Province and Guangzhou City.

© 2018 The Authors. Published by Elsevier B.V. This is an open access article under the CC BY-NC-ND license (<http://creativecommons.org/licenses/by-nc-nd/4.0/>).

1. Introduction

Over the last four decades, cardiac transplantation has been the best choice for patients with end-stage heart disease [1]. According to the International Society of Heart and Lung Transplantation (ISHLT), the median survival of cardiac transplantation patients is only 11 years. Moreover, for patients who survive the first year, the median survival rate is 13 years. Despite improvements in immunosuppression,

antibody-mediated rejection (AMR) still occurs and can result in death after transplantation [2].

AMR typically occurs when recipients were presensitized to donor antigens prior to operation or due to de novo donor-specific antibody (DSA) production post operatively. Complement cascade activation results in C4d deposition in interstitial vasculature [3], which is regarded as the best single marker of high specificity to diagnose AMR [4]. Moreover, C4d itself is an independent risk factor for cardiac allograft loss. A recent study reported that C4d-positive patients demonstrated a higher 3-year mortality of 67% and showed a positive association with cardiac allograft vasculopathy and panel-reactive antibody level [5]. This contributed to the identification of C4d as a prognostic factor for AMR. Early routine surveillance of C4d in cardiac transplantation had been strongly recommended by the ISHLT guidelines [6].

* Correspondence author at: 2693, Kaichuang Avenue, Huangpu District, Guangzhou, Guangdong 510630, China.

E-mail address: sunqiq@mail.sysu.edu.cn (Q. Sun).

¹ These authors contributed equally to this work.

Research in context

Evidence before this study

C4d is a specific biomarker for the diagnosis of antibody mediated cardiac allograft rejection and associated with >60% of life-threatening graft loss; however, it remains difficult to assess C4d noninvasively.

Added value of this study

We evaluated C4d deposition using targeted ultrasound and successfully obtained the qualitative images of C4d deposition in a wide cardiac allograft section, which, for the first time, reflected real-time C4d distribution. Moreover, normal intensity difference was used for quantitative analysis and exhibited an almost nearly linear correlation with the grade of C4d deposition according to the pathologic evidence.

Implications of all the available evidence

This noninvasive and quantitative approach for detecting C4d may prevent numerous patients from having to undergo an invasive biopsy.

However, the invasive nature of the current C4d detection method makes early routine surveillance difficult. At present, the detection of C4d relies on endomyocardial biopsy (EMB) for immunohistochemical or immunofluorescence staining [6]. Indeed, it is an invasive procedure and may cause a series of severe complications, such as coronary artery fistula, tricuspid regurgitation, and cardiac perforation, and can affect the patient's quality of life, particularly considering that the graft is beating [7]. In addition, the small piece of tissue obtained by EMB hardly reflects the C4d deposition within the global allograft [8]. Moreover, the traditional analysis method of C4d deposition only provides semi-quantitative data [9]. Thus, a method for visualizing C4d in a noninvasive, more representative, and quantitative manner is urgently needed for early AMR diagnosis.

Targeted ultrasound (US) is an imaging technology that has recently been developed to detect targets at the cellular and molecular levels and has an excellent sensitivity and specificity when applied as contrast-enhanced ultrasound (CEUS) [10]. Moreover, it has several practical advantages as a molecular imaging technique, including its low cost, real-time detection, and convenience over other imaging modalities, including computed tomography, nuclear imaging, X-ray and angiography [11]. Recently, intragraft T cells and intercellular adhesion molecule-1 expression had been successfully imaged using targeted US [12,13]. Considering the abundant expression of C4d on the capillary endothelium cells in cardiac allograft with acute AMR, it could be an ideal target for designing targeted microbubbles (MBs).

Therefore, in this study, we aimed to develop a novel approach for noninvasive, more representative, and quantitative evaluation of C4d deposition in a cardiac allograft rodent model.

2. Materials and methods

2.1. Experimental protocol

C4d-targeted MBs (MB_{C4d}) were prepared using the streptavidin-biotin conjugation system, and the AMR rat model with C4d deposition was established via pre-sensitization using skin transplantation, as

described below. At indicated time points, MB_{C4d} was injected into recipients. Qualitative and quantitative analyses were performed using the destruction-replenishment method and based on the targeted US imaging signal from MBs that were bound to C4d. Results were assessed using CEUS qualitative and quantitative analysis software (Fig. 1).

2.2. Preparations of MB_{C4d} and control MBs (MB_{con})

Streptavidin-coated MBs (MicroMarker™ Target Ready) were purchased from VisualSonics, Inc. (Toronto, Canada) which was commercially available. C4d antibodies (1 mg/mL, anti-Rat C4d Cat. No. HP8034; Hycult Biotech Inc., Plymouth Meeting, PA) were biotinylated in order to conjugate with streptavidin MBs before use. Biotinylated isotype-matched rabbit control immunoglobulin G (IgG) antibody (Jackson ImmunoResearch Laboratories, West Grove, PA) was used as a specific control. Two types of MBs (MB_{C4d} and MB_{con}) were prepared according to the manufacturer's instruction for the experiment. Briefly, after 1 ml of saline was injected into the MicroMarker™ Target Ready vial, gently agitated for 10 s and placed at room temperature 5 min, 50 µg of antibodies was injected into the vial and incubated for 20 min at room temperature with gentle shaking. Unconjugated ligand was removed by centrifugal washing. Then, 300 µl, which was confirmed to be the most appropriate dose by our early exploration study (Fig. S1), of dissolved MBs labeled with antibodies were applied per animal in cardiac transplant recipients.

In addition, FITC-labeled C4d antibody was used as reporter for ligand conjugation to MB surfaces. The fluorescence of FITC-MB_{C4d} was evaluated using a FACS Calibur flow cytometer (BD Biosciences, America), which calculated the combination rate of streptavidin MBs and biotinylated antibodies. MBs without C4d were used as negative control. Moreover, fluorescence microscopy was used to verify the combination of streptavidin MBs and biotinylated C4d antibodies.

2.3. Rat skin and cardiac transplantation

Adult male (200–250 g) Lewis and Brown Norway (BN) rats were obtained from Charles River Laboratories (Beijing, China) and were housed at Sun Yat-sen University. Animal experiments were approved by the Animal Committee of Sun Yat-sen University (Approve number: 1709044). In the presensitized group, Lewis rats received skin grafts on their dorsum from BN rats 2 weeks before cardiac transplantation. Briefly, full-thickness BN skin was grafted onto the dorsum of Lewis rats, and the skin allografts were rejected at 10.6 ± 2.7 days post-operation. All recipients presensitized in this fashion developed antidonor specific antibodies. At 2 weeks after skin transplantation, abdominal heterotopic cardiac transplantation was performed. Anesthesia was induced and maintained with isoflurane. After being anesthetized, the donor rat was heparinized (500 U/kg IV). A thoracotomy was then performed and the heart was exposed. The superior and inferior vena cava together with the pulmonary veins were ligated. The ascending aorta and pulmonary artery were cut and the explanted heart was immediately immersed in cold saline. The recipient rat was similarly anesthetized. The abdomen was opened by a midline incision, and the abdominal aorta and the vena cava were isolated and occluded with small vessel clamps. The ascending aorta and pulmonary artery of the donor heart were anastomosed end to side to the abdominal aorta and the vena cava of the recipient rat, respectively. After heart reperfusion, the abdomen was closed and the rat was allowed to recover. Allograft survival was determined by direct palpation and rejection was considered complete at cessation of a palpable heart beat. The allografts were collected at indicated time points (2 h, 4 h, 8 h, 1 day, 2 days, 3 days, 4 days, and 5 days post-operatively, $n = 5/\text{time point}$). The recipients were sacrificed by overdose of chloral hydrate following the allograft loss or collection of samples.

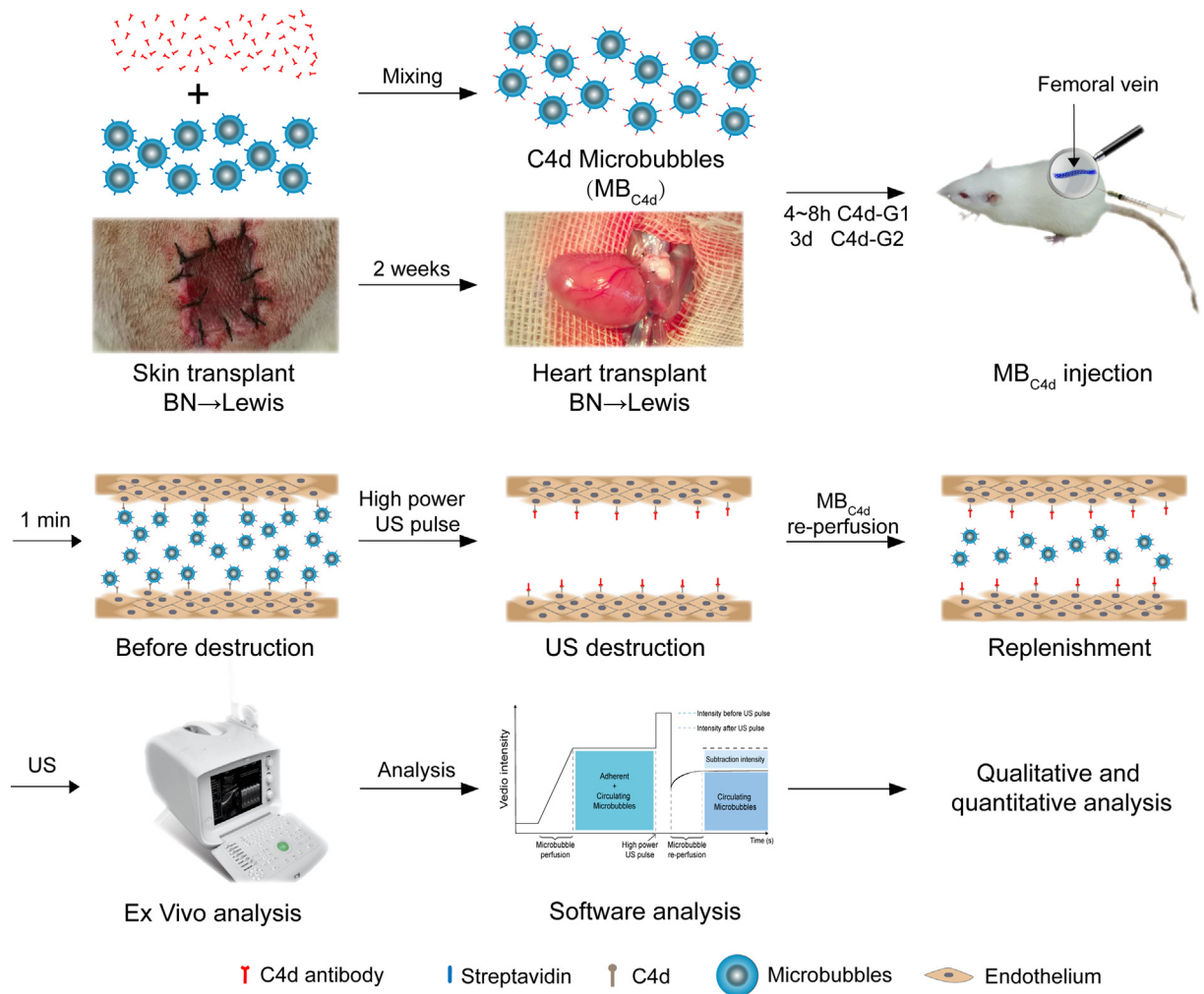


Fig. 1. Experimental protocol of noninvasive quantization of C4d deposition for the diagnosis of antibody-mediated cardiac allograft rejection using targeted microbubbles.

2.4. Detection of circulating DSAs

The serum of graft recipients was obtained at the indicated time point (days 0, 3, 7, 10, 14 after skin transplantation and day 1, 2, 3, 4, 5 after cardiac transplantation). Circulating donor-specific IgG and IgM antibodies were assessed by flow cytometry. In short, recipient sera were incubated with BN donor splenocytes at 37 °C for 30 min, washed, and then incubated with FITC-labeled anti-rat IgG (Abcam, Cambridge, England) and rhodamine red-conjugated anti-rat IgM (Jackson ImmunoResearch Laboratories, West Grove, PA) at 4 °C for 1 h. Cells were analyzed by flow cytometry with results expressed as the mean fluorescence intensity to reflect individual serum anti-donor antibody levels.

2.5. Histology and immunohistochemistry

Cardiac grafts were harvested at indicated time points illustrated above. Syngeneic grafts served as controls. Grafts were then formalin fixed and embedded in paraffin before staining with hematoxylin and eosin (H&E) and anti-C4d (0.1 mg/mL, anti-Rat C4d Cat. No. HP8034; Hycult Biotech Inc., Plymouth Meeting, PA), anti-CD68 (1:400; ab125212, Abcam), and anti-CD3 (1:400, ab16669, Abcam). Histologic changes and C4d staining in interstitial vascular tissue were examined by light microscopy.

2.6. Evaluation of C4d expression tissue with image-pro plus (IPP)

Expression levels of C4d were examined by immunohistochemistry, as described above. Quantitative analysis of C4d in tissues was performed using IPP 6.0 imaging software (Media Cybernetics, Silver Spring, MD, USA) (Fig. S2). Briefly, typical images of immunohistochemistry at 2088 × 1560 pixel resolution at 200× magnification were captured. Images were then sent to IPP. Images were first calibrated for intensity to generate a uniform level of intensity for all images. The entire image was analyzed, and only typical images were chosen for analysis. The area was set from 20 to 10,000,000 square pixels. The total integrated optical density (IOD) and area were determined for each image. The area of C4d was selected by an experienced pathologist and confirmed by another pathologist. Images were converted to gray scale when all or most of the C4d area was chosen, and values were counted.

2.7. Image acquisition for C4d evaluation

CEUS was performed using a clinical US imaging system (Logiq E9 digital premium ultrasound system, GE, Milwaukee, WI) and images of rat cardiac allografts were collected using a broadband ML6-15D high-frequency scope with the following imaging parameters: frequency of 10 MHz, gain of 20–30 dB, image depth of 2–3 cm, acoustic

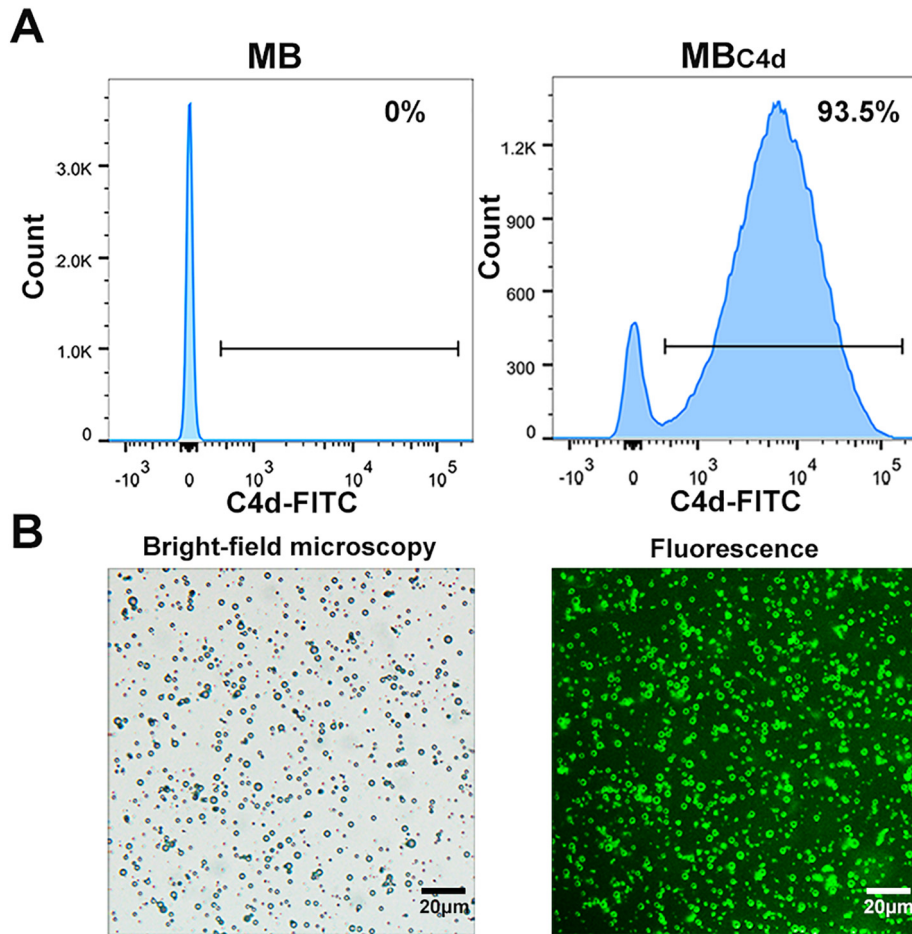


Fig. 2. Characteristic of C4d targeted microbubbles (MBs). Biotinylated C4d was labeled by FITC and subsequently conjugated to the MBs. (A) Fluorescence histogram for MBs and C4d bound MBs ($n = 5$). (B) Fluorescent microscopy showed conjugation of C4d to MBs with significant fluorescence signal on the MBs ($n = 5$).

output of 7%, dynamic range of 40–45 dB, and mechanical index of 0.09 at transection of the cardiac allograft. Section was fixed in the short axis of the left ventricular section to avoid the cardiac apex and mitral valve. Targeted US imaging was obtained via a destructive-replenishment approach. In short, all animals were injected with both MB_{Con} and MB_{C4d} via the femoral vein successfully and, after 1 min, pre-destruction images, which including sufficiently bound and free MBs were obtained. After that, all MBs in the sector were destroyed by “flash” US irradiation with a higher mechanical index of 0.24 for 1 s. Subsequent post-destruction images lasted for 10 s to capture only freely circulating MBs. All CEUS images were collected for further off-line quantitative analysis.

2.8. Establishment of qualitative targeted C4d US imaging and quantitative analysis

Qualitative and quantitative targeted US imaging signals from MBs that were bound to C4d were analyzed using the CEUS qualitative analysis software IDS and quantitative analyzing software Sonamath, respectively (both from Ambition T.C., Chongqing, China), as described previously [14]. The myocardium of the left ventricular short axis was outlined and set as the region of interest. The qualitative imaging signal intensity of attached MBs was calculated by subtracting the post-destruction gray scale signal of the region of interest from the pre-destruction one. The quantification of targeted US imaging signal was achieved using normalized intensity differences [NIDs (%) = pre-destruction signal intensity–post-destruction signal intensity / pre-destruction signal intensity]. That is, the ratio of the attached MBs

imaging signal intensity to the total MBs imaging signal intensity was calculated.

3. Statistics

The data software SPSS 20.0 (Chicago, Illinois, USA) was used for statistical analysis. All values are expressed as the mean \pm standard deviation. Kaplan–Meier curves and log-rank tests were used to compare the survival rates. Data were normally distributed and analyzed using Student’s *t*-test or a one-way analysis of variance. Significance was assumed when $p < .05$.

4. Results

4.1. Characterization of MB_{C4d}

The mean diameter of the targeted MBs was 1.3 μ m and the number of MB was 2×10^9 per ml [11]. The binding rate of MBs to C4d antibodies was $93.0 \pm 4.5\%$ (Fig. 2A). Furthermore, successful coupling of the C4d to the MBs surface was verified by flow epifluorescence (Fig. 2B).

4.2. Rat model of antibody-mediated cardiac allograft rejection accompanied with C4d deposition

To establish the model of antibody-mediated cardiac allograft rejection, we pre-sensitized the graft recipients with skin from BN donors 2 weeks before cardiac transplantation while the non-sensitized (NS) group was mainly recognized as acute cellular rejection. Allograft survival time in the pre-sensitized (PS) group was significantly reduced

compared to that of the NS group (5.2 ± 0.8 vs 8.8 ± 0.8 days, $p = .004$) (Fig. 3A). DSAs (IgG and IgM) after skin and cardiac transplantation were sequentially analyzed. In the PS group, the DSA-IgG level was gradually increased. At 2 weeks post skin transplantation, the IgG level

was significantly increased compared to normal level (564.6 ± 93.0 vs 119.3 ± 14.0 , $p < 0.001$). The DSA-IgM level was significantly elevated at 10 days (50.4 ± 2.9 vs 38.2 ± 2.6 days, $p = .012$) and decreased to normal at 14 days post skin transplantation, possibly through a rapid

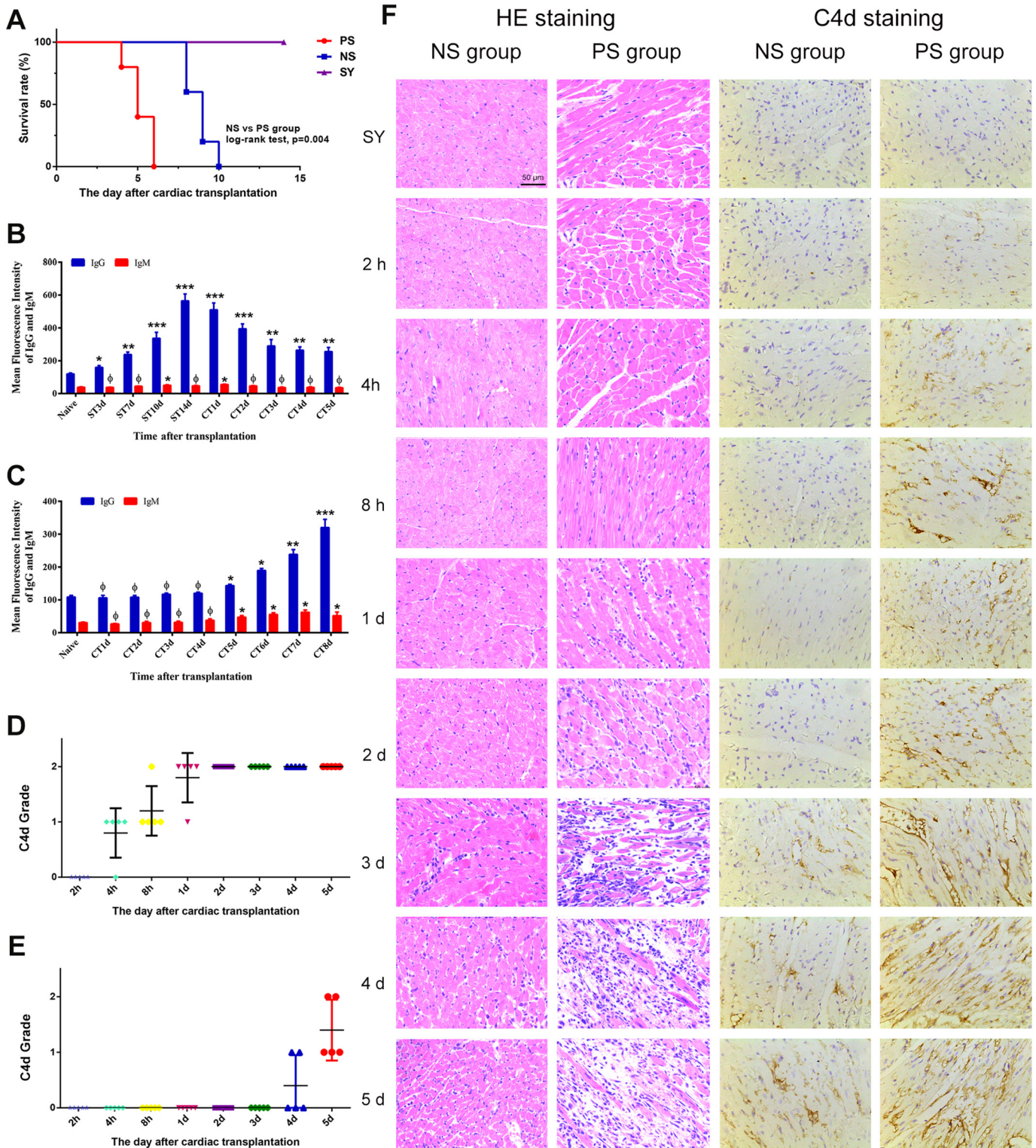


Fig. 3. Construction and characteristics verification of antibody-mediated rejection in a cardiac transplantation rat model. (A) Survival in the pre-sensitized (PS), non-prensensitized (NS), and syngeneic (SY) groups ($n = 5$ /group). (B) Changes in anti-donor specific antibody levels (DSA, IgG and IgM) after skin and cardiac transplantation in the PS group ($n = 5$). (C) Changes in DSA level (IgG and IgM) after cardiac transplantation in the NS group ($n = 5$). (D, E) The grades of C4d deposition in the PS and NS groups at indicated time points, respectively, evaluated by the semi-quantitative scoring criteria ($n = 5$ /time point). (F) Hematoxylin and eosin (H&E) and C4d staining of cardiac allografts in the NS and PS groups at different time points after cardiac transplantation. SY allografts served as control. ($n = 5$ /time point). Magnification: $400\times$; $*P < .05$, $**P < .01$, $***P < .001$; Φ , no significance; ST, skin transplantation; CT, cardiac transplantation.

breakdown of serum IgM. Our previous and other studies have also demonstrated that IgG is the major type of DSA which results in allograft rejection in animal models using skin pre-sensitization methods [15,16]. After cardiac transplantation, DSA-IgG levels decreased slightly, but were still significantly higher than normal, which may be due to the adsorption of grafts to DSA (Fig. 3B). In the NS group, both DSA-IgG and DSA-IgM were low until 4 days after cardiac transplantation and slightly increased from 5 days until graft loss (Fig. 3C). Then, histological features of cardiac allografts and C4d deposition in the PS and NS groups were observed at indicated time points post operatively. In the PS group, capillary inflammatory infiltrates, interstitial edema, and myocyte necrosis could be observed and were gradually aggravated over time. These histologic features conformed to the criteria of AMR. However, in the NS group, the histological features were mainly interstitial inflammation, and graft injuries were less severe compared to those observed in the PS group at the same time points. Moreover, the C4d deposition could be observed until 3 days after cardiac transplantation (Fig. 3F). Furthermore, C4d deposition was evaluated using semiquantitative scoring criteria according to the ISHLT: grade 0, <10% of all capillaries = negative; grade 1, 10%–50% of all capillaries = focal staining; grade 2, >50% of all capillaries = diffuse staining [9]. According to this standard, in the PS group, we determined that the C4d grade of all 10 syngeneic grafts and allografts 2 h after transplantation were grade 0 (G0), 8 of 10 allografts at 4–8 h after transplantation were grade 1 (G1), and 24 of 25 allografts at >1 day after transplantation were grade 2 (G2) (Fig. 3D). However, in the NS group, all allografts at 2 h to 3 days after transplantation were grade 0 (G0), 2 of 5 allografts at 4 days after transplantation were grade 1 (G1), and 2 of 5 allografts after 5 days after transplantation were grade 2 (G2) (Fig. 3E).

To further characterize this AMR animal model, we examined the phenotype of graft-infiltrating cells using immunohistochemistry with anti-CD68 and -CD3 antibodies to detect macrophages and T cells. The predominance of macrophages infiltrated grafts in the PS group, and substantial T cells rather than macrophages infiltrated grafts in the NS group. Moreover, the macrophages mainly infiltrated into the capillaries, whereas the infiltration of T cells was characterized as interstitial inflammation in the two groups (Fig. 4). We summarized these histological features in Table 1, according to the ISHLT criteria [9].

4.3. Qualitative analysis of the intragraft C4d deposition by targeted US

At 3 days post-transplantation in the syngeneic graft (C4d-G0) and at 4–8 h (C4d-G1) and 3 d (C4d-G2) post-transplantation in the allograft, MB_{Con} and MB_{C4d} were injected into recipients. The time interval between applications of MB_{Con} and MB_{C4d} was 30 min to ensure clearance of the MB_{Con} from circulation. The US imaging signal from MBs attached to C4d is expressed as the subtraction of MB densities before and after the destruction pulse according to the experimental protocol. As shown in Fig. 5, on receiving MB_{C4d}, much stronger molecular US imaging signals were observed in each group compared with that of the two control groups. Furthermore, the intensity signals of C4d were increased with the increase in C4d deposition according to the pathologic evidence. Moreover, the distribution of C4d signal showed non-uniform areas of strong and weak expression (Fig. 5).

4.4. Quantitative analysis of the intragraft C4d deposition by targeted US

As described in the methods, the NID was used as a parameter for quantitative analysis of C4d-targeted US imaging. The NID of the MB_{Con} group was $6.3 \pm 1.9\%$. The C4d-G0, C4d-G1 and C4d-G2 values were $6.3 \pm 1.4\%$, $13.2 \pm 2.1\%$, and $27.2 \pm 2.4\%$, respectively. Significant differences were observed between groups, and a significant correlation was found between NID and C4d grade ($r_s = 0.945$; $p < .01$) (Fig. 6A–B). To verify the accuracy of NID as a C4d quantitative analysis parameter, the IOD of C4d staining, as determined by microscopy, were also evaluated by IPP. As expected, the IOD followed the same pattern as the NID

across each C4d grade (Fig. 6C–D), which demonstrates the feasibility and accuracy of the NID as a method of quantitatively analyzing C4d deposition.

4.5. Safety evaluation

Death and heart rate changes were not observed during MB injection. Anorexia, slow activity, and weight loss were not observed after MB_{C4d} injection. Furthermore, we compared the survival and pathologic features of the cardiac allograft between the MB_{C4d} injection and Non-MB_{C4d} injection groups (Fig. S3). There was no significant difference in survival rate between these two groups (Fig. S3A). Moreover, at 3 days post operatively, we obtained the cardiac allografts, which were subjected to MB_{C4d} injection at 1 day after transplantation. The degrees of damage in these allografts were similar to the non-MB_{C4d} injection group (Fig. S3B).

5. Discussion

In this study, using US imaging based on MB_{C4d}, we developed an easy and novel approach to evaluate C4d deposition within a cardiac allograft. In doing so, we developed a noninvasive, more representative, and quantitative evaluation technique for this important biomarker. This simple approach may spare thousands of cardiac allograft recipients from undergoing invasive EMB for detecting C4d.

This study, for the first time, provided a noninvasive approach for intragraft C4d evaluation. Currently, the detection of intragraft C4d relies on EMB, which requires fluoroscopy guidance. Moreover, endomyocardial tissue is usually obtained percutaneously from the right or left ventricle via a peripheral vessel using biopsy forceps through a long sheath. Such a procedure is invasive, particularly when it is performed in a beating heart [17]. Conversely, targeted US imaging only requires an ultrasonic test after intravenous injection of MBs. There was no need for direct contact and invasive manipulation for the cardiac allograft [18], which would provide higher acceptance to recipients and doctors. Thus, the non-invasive C4d-targeted US imaging will make routine surveillance of intragraft C4d possible.

This approach also demonstrated, for the first time, a method to evaluate C4d deposition in a whole section within the cardiac graft. Due to C4d being located within capillaries, C4d deposition will vary in accordance with capillary distribution [19]. In specimens obtained by EMB, focal C4d depositions are often observed [20]. Thus, the sampling error of the small pieces of tissues obtained by EMB could be expected, which is a real problem and may result in a false negative diagnosis [21]. Targeted US can visualize the entire myocardium in a whole section of the allograft to evaluate the deposition, which markedly increased the accuracy of C4d diagnosis. This study provided the first image that showed the distribution of C4d in a whole allograft section. As shown in Fig. 5, C4d deposition in the cardiac allograft was indeed quite non-uniform, which may be consistent with the non-uniform distribution of intramyocardial capillaries. This feature in turn suggested that the sample error of EMB is inevitable. Thus, C4d-targeted US imaging, in comparison with EMB, could significantly decrease the sample error, and provided a more accurate C4d evaluation globally.

Moreover, another advantage of this novel approach was the ability to develop a quantitative C4d analysis technique using an objective indicator, which will produce a reliable result. Traditional methods for analyzing C4d deposition provides only semiquantitative data that depend on the pathologist's subjective judgment [22]. In this study, an objective indicator, NID, which was calculated using the destruction-replenishment method, was used for quantitative analysis of C4d deposition. The application of the objective indicator will be of great value for avoiding bias across pathologists as its magnitude reflects the intensity of C4d deposition. The NIDs in the positive groups were significantly higher compared to the syngeneic and MB_{con}-injected control groups

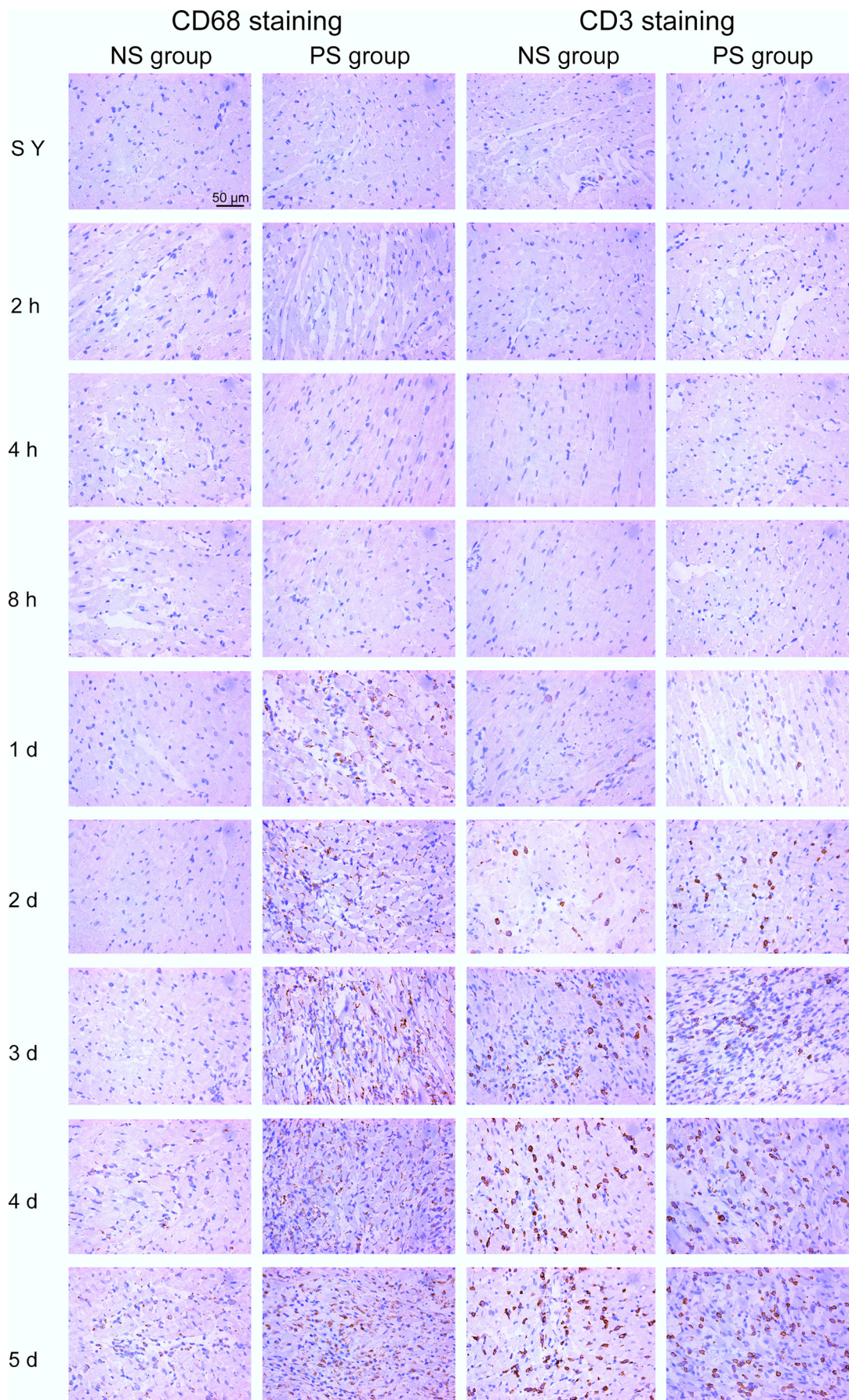


Fig. 4. CD68 and CD3 staining of cardiac allografts at indicated time points. CD68 and CD3 staining of cardiac allograft in the nonpresensitized (NS) and presensitized (PS) groups at different time points after cardiac transplantation, syngeneic (SY) allografts served as control (n = 5/time point). Magnification: 400×.

Table 1
Histological evaluation according to the criteria of ISHLT.

Histology		Time after cardiac transplantation							
		2 h	4 h	8 h	1d	2d	3d	4d	5d
Capillary C4d distribution (grade)	NS	0	0	0	0	0	0.4 ± 0.5	0.6 ± 0.5	1.4 ± 0.5
	PS	0	0.8 ± 0.4	1.2 ± 0.4	1.8 ± 0.4	2	2	2	2
Intravascular CD68 distribution (grade)	NS	0	0	0	0	0	0.4 ± 0.5	1.0 ± 0.7	2
	PS	0	0	0	0.6 ± 0.5	1.6 ± 0.5	2	2	2
Intravascular activated mononuclear cells	NS	-	-	-	-	+	+	+	+
	PS	-	-	+	+	+	+	+	+
Interstitial edema	NS	-	-	-	-	-	-	-	+
	PS	-	-	-	-	+	+	+	+
Hemorrhage	NS	-	-	-	-	-	-	-	-
	PS	-	-	-	-	-	+	+	+
Necrosis	NS	-	-	-	-	-	-	-	-
	PS	-	-	-	-	-	+	+	+
Vascular thrombosis	NS	-	-	-	-	-	-	-	-
	PS	-	-	-	-	-	+	+	+

Abbreviations: ISHLT, International Society of Heart and Lung Transplantation; NS, nonpresensitized; PS, presensitized; -, negative; +, positive. The scoring criteria of C4d deposition and intravascular CD68 distribution: grade 0, <10% of all capillaries; grade 1, 10%–50% of all capillaries; grade 2, >50% of all capillaries. Data are mean ± standard deviation. Histological evaluations were performed using light microscopy by an independent observer, who was blinded to the experimental conditions.

and had a linear correlation with the grade of C4d deposition. The intensity signals of C4d and NIDs were increased with the increase in C4d deposition according to the pathologic evidence. Moreover, as targeted US

is sufficiently sensitive to detect single MB in the bloodstream, NID accurately reflects the number of MBs bound to C4d in situ. Focal and weak C4d deposition could be visualized at 4 h post operative,

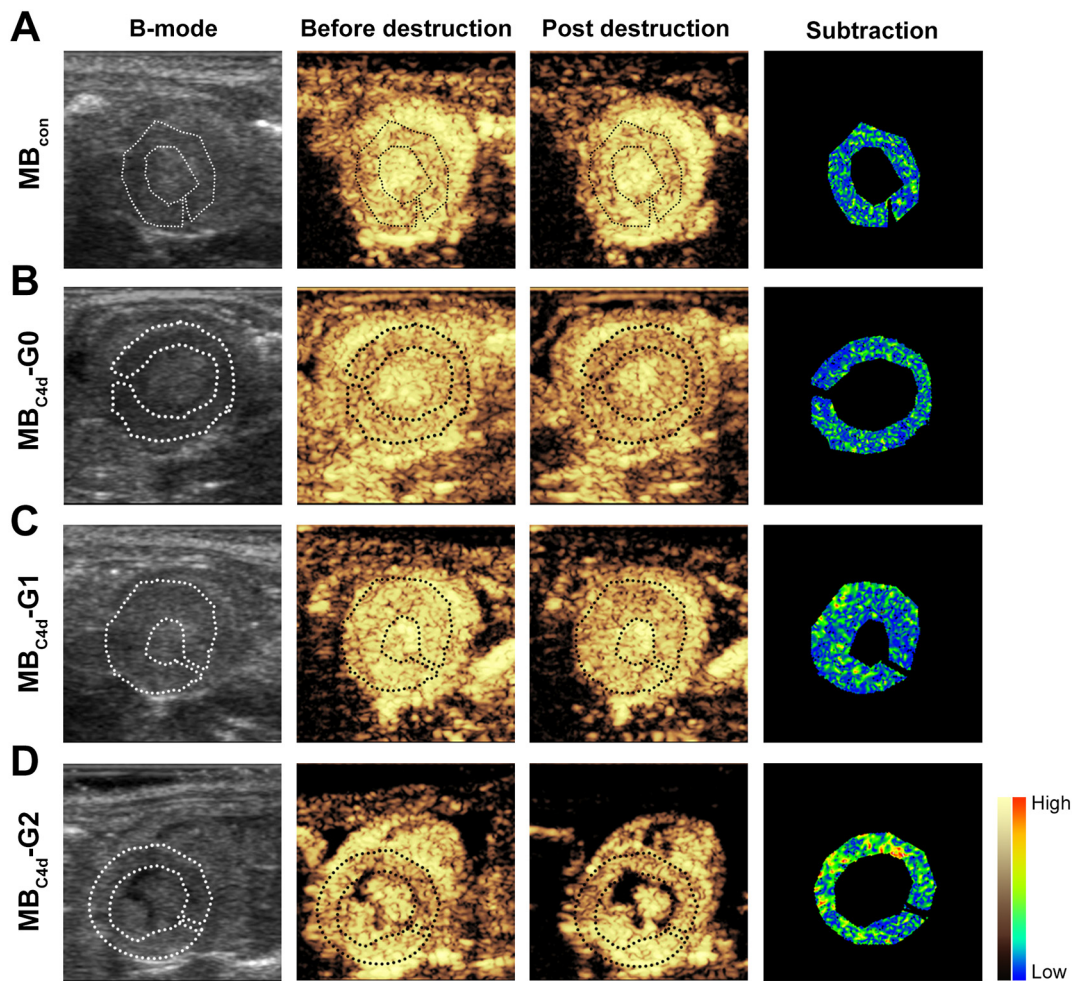


Fig. 5. Representative image of qualitative analysis of C4d in the cardiac allograft. The ultrasound (US) imaging signal from microbubbles (MBs) attached to C4d is expressed as the subtraction of the MB densities before and after the destruction pulse. Images in each group are ultrasound B-mode images, contrast-enhanced ultrasound (CEUS) images before destruction, CEUS image after destruction, and subtracted image by IDS, respectively. The myocardial area was outlined by a dotted line. (A–D) Representative targeted US imaging of the MB_{con} group (n = 15), MB_{C4d-G0} group (syngeneic grafts 3 d after transplantation; n = 5), MB_{C4d-G1} group (4–8 h after transplantation; n = 5) and MB_{C4d-G2} group (3 d after transplantation; n = 5).

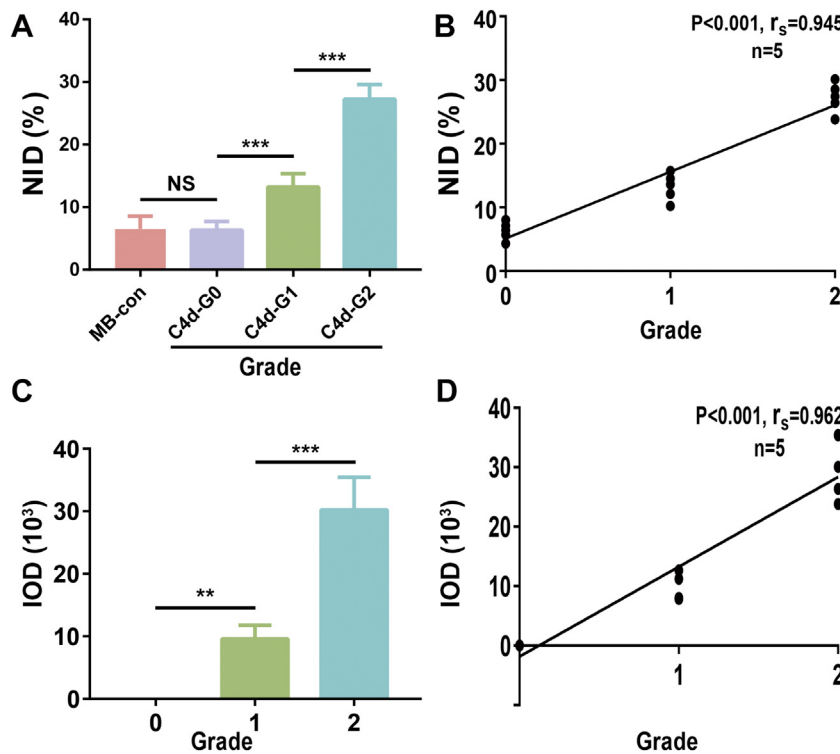


Fig. 6. Quantitative analysis and results of C4d deposition in the cardiac allografts. (A) The normalized intensity difference (NID) results of different C4d grades ($n = 15$ in the MB_{con} group; $n = 5$ in each of other groups). (B) Correlation analysis between NID and C4d grades ($n = 5$ /group). (C) The integrated optical density (IOD) results of different C4d grades, as evaluated by Image-Pro Plus ($n = 5$ /group). (D) Correlation analysis between IOD and C4d grades ($n = 5$ /group). ** $P < .01$; *** $P < .001$.

suggesting that NID is sensitive enough to catch early weak C4d signals. To verify the accuracy of NID as a C4d quantitative analysis parameter, the IOD of C4d staining, as detected by microscopy, were also evaluated using IPP [23]. As expected, the IOD agreed with the C4d grade that was acquired from NIDs, which demonstrates the feasibility and accuracy of using NID as a quantitative analysis for C4d deposition.

Recently, the importance of AMR has well been recognized for its association with severe coronary arteriosclerosis and allograft dysfunction [24–27]. Thus, routine surveillance of C4d is of great value in improving recipient outcomes. According to a recent report [5], as much as 42.9% of AMR cases were subclinical, as indicated by a normal allograft function and positive C4d deposition. Furthermore, this was closely associated with allograft loss. The noninvasive and easily performed features of C4d-targeted US imaging make routine C4d surveillance much more convenient, which increases the likelihood of patients with subclinical AMR receiving timely treatment and achieving a better prognosis. Furthermore, this approach could potentially be used to simultaneously assess AMR and graft function, which helped to identify the cause of graft dysfunction. In addition, although C4d are often bound on the surface of endothelial cell covalently, C4d loss as early as 8 days after treatment of AMR has been reported [19,28]. Therefore, real-time C4d-targeted US can facilitate the monitoring of treatment efficacy. In addition to cardiac transplantation, C4d deposition is of great value in diagnosis and treatment of renal transplant rejection, liver transplant rejection, autoimmune diseases, certain types of kidney disease, and tumors [4]. This method might also be used to diagnose these diseases noninvasively.

To date, targeted US imaging has been applied in human clinical practice in various types of cancer and has shown good accuracy and safety [18,29]. In this study, death and heart rate changes were not observed during MB injection. Anorexia, slow activity, and weight loss were not observed after MB_{C4d} injection. We also demonstrated that MB_{C4d} injection did not affect the allograft survival and aggravate injury, which demonstrated the safety of MB_{C4d} injection.

As CEUS has been widely used in clinical settings, the technology of C4d-targeted US imaging is expected to be applied quickly to clinical

practice. However, before performing clinical trials, the immunogenicity of streptavidin-based conjugated MB and antibodies require testing. Furthermore, the injection doses of targeted MBs, destruction time, and positive judgment standards must be robustly identified. Nevertheless, the functionalization of MB via covalently integrated binding epitopes could be designed for further clinical use [30]. Three-dimensional contrast-enhanced imaging is now available for human use, but there is a lack of commercially available ultrasound systems for high-frequency preclinical three-dimensional contrast imaging and its complex operation [11]. To facilitate clinical promotion, we used two-dimensional contrast-enhanced system to evaluate C4d deposition. Conditional units could use three-dimensional imaging technology to evaluate C4d deposition in the global allograft.

It cannot be ignored that C4d is insufficient for pathological diagnosis of AMR, although it was regarded as the best single marker currently, because of its high specificity but low sensitivity. CD68⁺ macrophages that infiltrated the capillaries is another important histologic feature in AMR. We are designing CD68-targeted MBs and detecting macrophages by CEUS. We deduce that combined C4d and CD68 detection by CEUS would significantly improve the sensitivity of AMR diagnosis.

Overall, this study documents herein a noninvasive, more representative, and quantitative method for detecting C4d deposition in cardiac allografts in patients with AMR using C4d-targeted US imaging. Thus, the utility of this approach may realize noninvasive detection of this important biomarker in clinic.

Sources of funding

This work was supported by National Natural Science Foundation of China (Nos. 81770753, 81470978, 81371554 and 81601512), National Natural Science Foundation of Guangdong Province (No. 2015A030311040), Leading Scientific, Technical, and Innovation Talents of Guangdong special support program (No. 2015TX01R112), Science and Technology Project of Guangdong Province (No. 2015B020226005),

and Science and Technology Project of Guangzhou City (No. 201604020086).

Declaration of interests

The authors have no financial declare.

Author contributions

QQ.S, J.R designed the experiments. T.L., X.N.L., H.J.Z., H.F.Z., X.J.L., Y.Z., F.H., and T.Y. performed the experiments. H.F.Z. analyzed the data. T.L. edited the paper.

Appendix A. Supplementary data

Supplementary data to this article can be found online at <https://doi.org/10.1016/j.ebiom.2018.10.061>.

References

- [1] Dhital KK, Iyer A, Connellan M, et al. Adult heart transplantation with distant procurement and ex-vivo preservation of donor hearts after circulatory death: a case series. *Lancet* 2015;385(9987):2585–91.
- [2] Chambers DC, Yusef RD, Cherikh WS, et al. The registry of the international society for heart and lung transplantation: thirty-fourth adult lung and heart-lung transplantation report-2017; focus theme: allograft ischemic time. *J Heart Lung Transplant* 2017;36(10):1047–59.
- [3] Colvin RB, Smith RN. Antibody-mediated organ-allograft rejection. *Nat Rev Immunol* 2005;5(10):807–17.
- [4] Cohen D, Colvin RB, Daha MR, et al. Pros and cons for C4d as a biomarker. *Kidney Int* 2012;81(7):628–39.
- [5] Husain AN, Mirza KM, Fedson SE. Routine C4d immunohistochemistry in cardiac allografts: long-term outcomes. *J Heart Lung Transplant* 2017;36(12):1329–35.
- [6] Kobashigawa J, Crespo-Leiro MG, Ensminger SM, et al. Report from a consensus conference on antibody-mediated rejection in heart transplantation. *J Heart Lung Transplant* 2011;30(3):252–69.
- [7] Saraiva F, Matos V, Goncalves L, Antunes M, Providencia LA. Complications of endomyocardial biopsy in heart transplant patients: a retrospective study of 2117 consecutive procedures. *Transplant Proc* 2011;43(5):1908–12.
- [8] Fischer K, Ohori S, Meral FC, et al. Testing the efficacy of contrast-enhanced ultrasound in detecting transplant rejection using a murine model of heart transplantation. *Am J Transplant* 2017;17(7):1791–801.
- [9] Berry GJ, Burke MM, Andersen C, et al. The 2013 International Society for Heart and Lung Transplantation Working Formulation for the standardization of nomenclature in the pathologic diagnosis of antibody-mediated rejection in heart transplantation. *J Heart Lung Transplant* 2013;32(12):1147–62.
- [10] Unnikrishnan S, Klivanov AL. Microbubbles as ultrasound contrast agents for molecular imaging: preparation and application. *AJR Am J Roentgenol* 2012;199(2):292–9.
- [11] Hyvelin JM, Tardy I, Arbogast C, et al. Use of ultrasound contrast agent microbubbles in preclinical research: recommendations for small animal imaging. *Invest Radiol* 2013;48(8):570–83.
- [12] Weller GE, Lu E, Csikari MM, et al. Ultrasound imaging of acute cardiac transplant rejection with microbubbles targeted to intercellular adhesion molecule-1. *Circulation* 2003;108(2):218–24.
- [13] Grabner A, Kentrup D, Pawelski H, et al. Renal contrast-enhanced sonography findings in a model of acute cellular allograft rejection. *Am J Transplant* 2016;16(5):1612–9.
- [14] Qiu C, Yin T, Zhang Y, Lian Y, You Y, Wang K, et al. Ultrasound Imaging based on molecular targeting for quantitative evaluation of hepatic ischemia-reperfusion injury. *Am J Transplant* 2017;17(12):3087–97.
- [15] Liao T, Xue Y, Zhao D, et al. In vivo attenuation of antibody-mediated acute renal allograft rejection by ex vivo TGF-beta-induced CD4(+)Foxp3(+) regulatory T cells. *Front Immunol* 2017;8:1334.
- [16] Kohei N, Tanabe T, Horita S, et al. Sequential analysis of donor-specific antibodies and pathological findings in acute antibody-mediated rejection in a rat renal transplantation model. *Kidney Int* 2013;84(4):722–32.
- [17] Chimenti C, Frustaci A. Contribution and risks of left ventricular endomyocardial biopsy in patients with cardiomyopathies: a retrospective study over a 28-year period. *Circulation* 2013;128(14):1531–41.
- [18] Abou-Elkacem L, Bachawal SV, Willmann JK. Ultrasound molecular imaging: moving toward clinical translation. *Eur J Radiol* 2015;84(9):1685–93.
- [19] Minami K, Fau Murata K, Lee CY, Fau Lee Cy, Fox-Talbot K, et al. C4d deposition and clearance in cardiac transplants correlates with alloantibody levels and rejection in rats. *Am J Transplant* 2006;6(5 Pt 1):923–32.
- [20] Bruneval P, Angelini A, Miller D, et al. The XIIIth Banff conference on allograft pathology: the Banff 2015 heart meeting report: improving antibody-mediated rejection diagnostics: strengths, unmet needs, and future directions. *Am J Transplant* 2017;17(1):42–53.
- [21] Cooper LT, Fau Baughman KI, Feldman AM, Fau Feldman Am, Frustaci A, et al. The role of endomyocardial biopsy in the management of cardiovascular disease: a scientific statement from the American Heart Association, the American College of Cardiology, and the European Society of Cardiology. *Circulation* 2007;116(19):2216–33.
- [22] Moseley EL, Fau Atkinson C, Sharples LD, Fau Sharples Ld, Wallwork J, Fau Wallwork J, et al. Deposition of C4d and C3d in cardiac transplants: a factor in the development of coronary artery vasculopathy. *J Heart Lung Transplant* 2010;29(4):417–23.
- [23] Horai Y, Kakimoto T, Takemoto K, Tanaka M. Quantitative analysis of histopathological findings using image processing software. *J Toxicol Pathol* 2017;30:351–8.
- [24] Loupy A, Toquet C, Rouvier P, et al. Late failing heart allografts: pathology of cardiac allograft vasculopathy and association with antibody-mediated rejection. *Am J Transplant* 2016;16(1):111–20.
- [25] Clerkin KJ, Restaino SW, Zorn E, Vasilescu ER, Marboe CC, Mancini DM. The effect of timing and graft dysfunction on survival and cardiac allograft vasculopathy in antibody-mediated rejection. *J Heart Lung Transplant* 2016;35(9):1059–66.
- [26] Hodges AM, Lyster H, McDermott A, et al. Late antibody-mediated rejection after heart transplantation following the development of de novo donor-specific human leukocyte antigen antibody. *Transplantation* 2012;93(6):650–6.
- [27] Coutance G, Ouldamar S, Rouvier P, et al. Late antibody-mediated rejection after heart transplantation: mortality, graft function, and fulminant cardiac allograft vasculopathy. *J Heart Lung Transplant* 2015;34(8):1050–7.
- [28] Collins AB, Fau Schneeberger Ee, Pascual MA, Fau Pascual Ma, Saidman SL, et al. Complement activation in acute humoral renal allograft rejection: diagnostic significance of C4d deposits in peritubular capillaries. *J Am Soc Nephrol* 1999;10(10):2208–14.
- [29] Kiessling F, Fokong S, Bzyl J, Lederle W, Palmowski M, Lammers T. Recent advances in molecular, multimodal and theranostic ultrasound imaging. *Adv Drug Deliv Rev* 2014;72:15–27.
- [30] Willmann JK, Bonomo L, Carla Testa A, et al. Ultrasound molecular imaging with BR55 in patients with breast and ovarian lesions: first-in-human results. *J Clin Oncol* 2017;35(19):2133–40.